Journal of Applied Polymer Science

POSS-based fluorinated azobenzene-containing polymers: Photo-responsive behavior and evaluation of water repellency

Liang Chen,[1] Chuanglong He,[1] Yangen Huang,[1] Jianbao Huang,[1] Yanzhong Zhang,[1] Yu Gao[2]

[1]College of Chemistry, Chemical Engineering and Biotechnology, Donghua University, 2999 North Renmin Road, Shanghai 201620, China

[2]Research Institute of Donghua University, 2999 North Renmin Road, Shanghai 201620, China

Correspondence to: Y. Gao (gaoyu@dhu.edu.cn)

ABSTRACT: The photoresponsive polyhedral oligomeric silsesquioxanes (POSS) based fluorinated azobenzene-containing polymers were prepared and characterized by NMR, FT-IR, GPC, XRD, TG and UV–Vis spectra. The thermal property of the polymers was improved by the introduction of POSS cage. The *trans-cis* photoisomerization of the polymers in solution was similar to that of the fluorinated azobenzene monomer and in accordance with the first-order reaction kinetics equation within the first 250 seconds UV irradiation. The cotton fabrics coated with the polymers showed excellent water repellency and possessed switchable wettability under UV irradiation. © 2016 Wiley Periodicals, Inc. J. Appl. Polym. Sci. **2016**, *133*, 43540.

KEYWORDS: functionalization of polymers; nanostructured polymers; properties and characterization

Received 23 November 2015; accepted 16 February 2016

DOI: 10.1002/app.43540

INTRODUCTION

In the past decades, the wettability of stimuli-responsive surfaces controlled by external environmental variations including pH,[1] temperature,[2] electrical voltage,[3,4] and light irradiation,[5–8] have aroused great attentions because of their tremendous potential in both fundamental research and practical application.[9] Among above-mentioned stimuli, the innocuous and noninvasive nature of light irradiation makes it attractive to develop wettability switchable surfaces.[10] The low energy *trans*-isomeric state of azobenzene-containing compounds can be switched reversibly to *cis*-isomeric state upon exposure to UV light resulting in a change of surface wettability.[11] A variety of monomer layers and polymer surfaces with azobenzene group in either backbone or side chain were reported,[12–16] but few has been reported on polyhedral oligomeric silsesquioxanes (POSS) based azobenzene-containing polymers with fast photoresponse.

POSS, the well defined organic–inorganic hybrid compounds with inorganic cubic core and outer organic groups,[17] are the amazing building block for polymer composites in engineering materials, biological and electronic applications[18–20] due to their outstanding mechanical and thermal performance of the inorganic silica core and feasible modification of the corner organic functional groups. Moreover, the water and oil repellency of surfaces can be significantly increased by the long-chain perfluoroalkyl modified POSS compared with their pristine materials.[21,22] However, molecules containing perfluoroalkyl long-chain (C_nF_{2n+1}, $n \geq 8$) could result in a potential risk for human health and environmental concerns because of their accumulation in wildlife and human body.[23,24]

In this study, we prepared and characterized the functional POSS-based fluorinated azobenzene-containing polymers which were expected to be applied to photoresponsive surface with controlled wettability. Compared to long-chain perfluoroalkyl groups, the short ones are much less toxic,[25,26] so the semi-perfluorinated compound with short-chain perfluoroalkyl group (C_4F_9) was used in our study. Herein, the synthesis of fluorinated azobenzene-containing monomer and the POSS-based terpolymers, and their characterization as well as photoresponsive properties are described in detail. The photoswitchable wettability of cotton fabrics coated with polymers and the influences of POSS on it are also presented here.

EXPERIMENTAL

Materials

Octavinyl polyhedral oligomeric silsesquioxane (Ov-POSS) (99%) was purchased from Shenyang Meixi Fine Chemicals Co., Ltd (Shenyang, China) and dried under vacuum before use. 3,3,4,4,5,5,6,6,6-nonafluorohexan-1-ol (Shanghai Qinba Chemical Co., Ltd., China) was used as received. All other chemicals were purchased from Sinopharm Chemical Reagent Co., Ltd. (Shanghai, China). Methyl methacrylate (MMA) was distilled

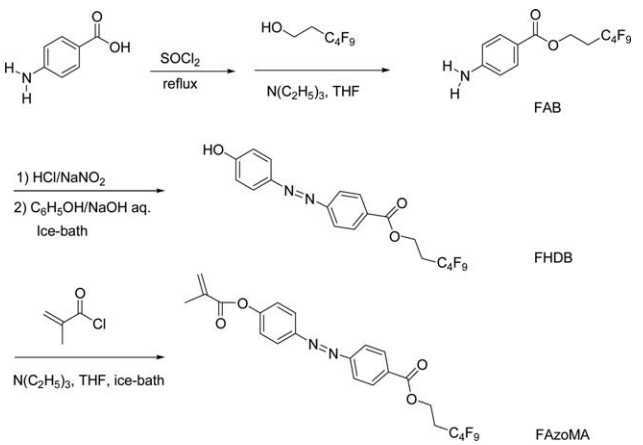

Scheme 1. Synthesis of FAzoMA.

from calcium hydride under vacuum before use. 2,2-Azobisisobutyronitrile (AIBN) was recrystallized from ethanol. Tetrahydrofuran (THF) was distilled from sodium/benzophenone immediately before use. Other chemicals were used as received.

Monomer Synthesis

Synthesis of 3,3,4,4,5,5,6,6,6-Nonafluorohexyl 4-Aminobenzoate (FAB). FAB was synthesized according to a reported method[27] as shown in Scheme 1. Firstly, 4-aminobenzoic acid (3 g, 21.9 mmol) was dissolved in thionyl chloride and refluxed for 4 hours under nitrogen atmospheres. The excess thionyl chloride was completely removed by reduced pressure distillation to obtain 4-aminobenzoyl chloride. Subsequently, 3,3,4,4,5,5,6,6,6-nonafluorohexan-1-ol (6 g, 22.7 mmol) was dissolved in dry THF (10 mL) and 4 mL triethylamine was added into the solution under nitrogen in an ice-bath. Then the obtained 4-aminobenzoyl chloride was dissolved in 10 mL dry THF and added dropwise into the reaction solution. The crude reaction mixture was stirred in ice-bath for four hours followed by filtration. The filtrate was concentrated and purified by chromatography using a column with silica gel. ^{1}H NMR ($CDCl_3$, 400.0 MHz), δ (ppm): 2.54 $\sim$ 2.86 (m, 2H, Ha), 4.13 (broad, 2H, He), 4.59 (t, $J = 6.4$ Hz, 2H, Hb), 6.66 (d, $J = 8.0$ Hz, 2H, Hd), 7.87(d, $J = 8.4$ Hz, 2H, Hc). ^{19}F NMR ($CDCl_3$, 377.0 MHz), δ (ppm): $-126.06 \sim -125.95$ (m, 2F), $-124.54 \sim -124.49$ (m, 2F), $-113.89 \sim -113.71$ (m, 2F), $-81.08 \sim -81.01$ (m, 3F).

Synthesis of 3,3,4,4,5,5,6,6,6-nonafluorohexyl4-[(4-Hydroxyphenyl)diazenyl]Benzoate (FHDB). FHDB was synthesized by a process starting from diazotization of FAB, followed by coupling reaction.[28] Briefly, FAB (2.0 g, 5.2 mmol) was mixed with 30 mL 2M HCl aqueous solution in 250 mL flask, and the mixture was constantly stirring in ice-bath until it was completely dissolved. Then $NaNO_2$ (0.4 g, 5.8 mmol) in 10 mL deionized water was added dropwise into the solution, and the solution changed from colorless to slight yellow. After stirring for another 30 min in ice-bath, phenol (0.55 g, 5.9 mmol) in 30 mL 1M cold NaOH aqueous solution was slowly added into above diazonium salt solution. The coupling reaction was accomplished in less than one hour when the yellowish-brown slurry formed. Then the precipitation was filtered off and dried at 60 °C under vacuum. The crude product was purified by silica gel column chromatography and the orange-yellow FHDB was obtained. ^{1}H NMR ($CDCl_3$, 400.0 MHz), δ (ppm): 2.62 $\sim$ 2.74 (m, 2H, Ha), 4.69 (t, $J = 6.4$ Hz, 2H, Hb), 5.43 (broad, 1H, Hg), 7.00 (d, $J = 8.8$ Hz, 2H, Hf), 7.93(d, 4H, $J = 8.4$ Hz, Hd, He), 8.19 (d, $J = 8.4$ Hz, 2H, Hc). ^{19}F NMR ($CDCl_3$, 377.0 MHz), δ (ppm): $-126.06 \sim -125.91$ (m, 2F), $-124.49 \sim -124.41$ (m, 2F), $-113.81 \sim -113.69$ (m, 2F), $-81.03 \sim -80.97$ (m, 3F).

Synthesis of 3,3,4,4,5,5,6,6,6-Nonafluorohexyl 4-{[4-(methacryloyloxy)phenyl]diazenyl}Benzoate (FAzoMA). The as-synthesized FHDB was further reacted with methacryloyl chloride to prepare the polymerizable fluorinated azobenzene-containing monomer. Typically, an oven-dried 100 mL Schlenk tube was charged with FHDB (1.5 g, 3.1 mmol), then the tube was degassed and flushed with nitrogen for three times. THF (10 mL) and triethylamine (0.46 g, 4.6 mmol) was transferred into the Schlenk tube by using gas-tight syringe. The mixture was allowed to stir in an ice-bath until the solution became homogeneous. A solution of methacryloyl chloride (0.50 g, 4.8 mmol) in THF (5 mL) was added slowly to the above solution. The reaction was maintained at 0 °C for one hour and monitored by thin-layer chromatography. The insoluble residue was removed by filtration and the filtrate was concentrated and purified by chromatography to get an orange-yellow powder. The monomer was further purified by recrystallization from ethanol and denoted as **FAzoMA**. ^{1}H NMR ($CDCl_3$, 400.0 MHz), δ (ppm): 2.11(s, 3H, Hh), 2.61 $\sim$ 2.73 (m, 2H, Ha), 4.70 (t, $J = 6.4$ Hz, 2H, Hb), 5.83 (s, 1H, Hg), 6.42 (s, 1H, Hg), 7.34 (d, $J = 4.6$ Hz, 2H, Hf), 7.98 (d, $J = 4.2$ Hz, 2H, He), 8.04(d, $J = 4.4$ Hz, 2H, Hd), 8.21 (d, $J = 4.4$ Hz, 2H, Hc). ^{19}F NMR ($CDCl_3$, 377.0 MHz), δ (ppm): $-126.01 \sim -125.90$ (m, 2F), $-124.48 \sim -124.41$ (m, 2F), $-113.81 \sim -113.69$ (m, 2F), $-81.03 \sim -80.96$ (m, 3F).

Polymer Preparation

In a typical polymerization procedure (seen in Scheme 2), Ov-POSS at desired amount were added into 50 mL Schlenk tube. The tube was degassed and filled with N_2, followed by adding THF (4 mL), MMA (1.2 g, 12 mmol), **FAzoMA** (1.5 g,

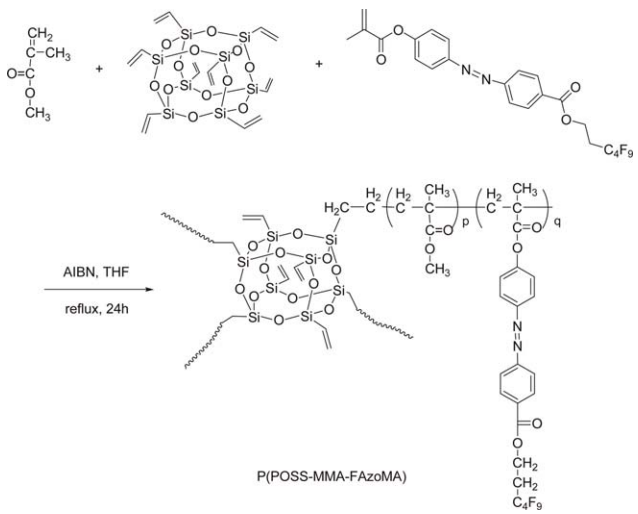

Scheme 2. Synthesis of POSS-based terpolymer.

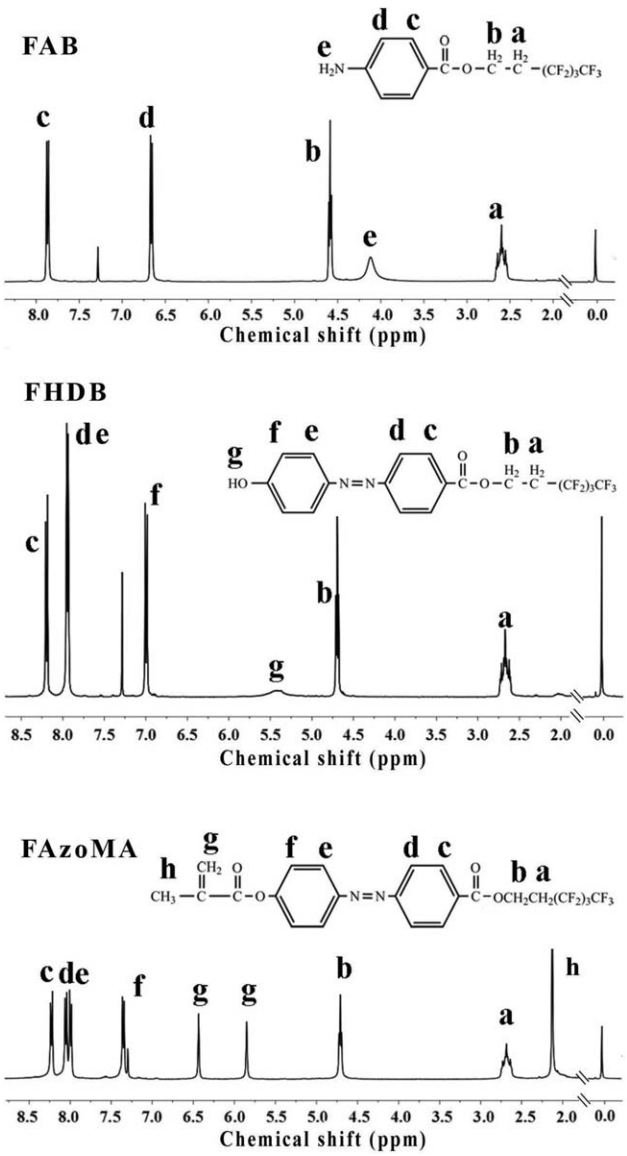

Figure 1. ^{1}H NMR spectra of FAB, FHDB and **FAzoMA**.

2.7 mmol) in THF (4 mL) and 1 wt % AIBN relative to monomers. Then the Schenk tube was immersed into a 70 °C pre-set oil bath and the monomers were allowed to polymerize under N_2 atmosphere and under dark with stirring for 24 hours followed by purification procedure. The crude product was purified by several cycles of dissolve-precipitation by applying chloroform/ethanol (v/v = 1/30) solution as precipitant because the polymers precipitated in it while the small amount of Ov-POSS dissolved. The polymers were finally dried under vacuum at 60 °C to an orange-red powder of constant weight. The polymers with different amount of POSS were labeled by **P0**, **P50**, **P100**, respectively.

Cotton Fabric Treatment

The cotton fabrics were desized, bleached and cleaned in advance. Then the cotton fabrics (3 cm × 10 cm) were soaked in the 0.01 g/mL polymers solution (THF as solvent) for 2 h, and then were dried at 80 °C for one hour and cured at 160 °C for 3 min.

Characterization

^{1}H, ^{19}F, and ^{29}Si NMR spectra were recorded at ambient temperature on Bruker AV400 operating at 400.0, 377.0, and 79.6 MHz, respectively. Tetramethylsilane (TMS) was applied as the internal chemical shift reference for ^{1}H NMR spectra and $CFCl_3$ as an external standard for ^{19}F NMR spectra. FT-IR spectra were recorded on a FT-IR spectrometer (Avatar 380) using KBr crystal in the infrared region 4000 ∼ 400 cm^{-1}. Gel permeation chromatography (GPC) analysis was carried out in THF at 35 °C with a flow rate of 1.0 mL/min using a Waters 1515 system fitted with Waters 2414 differential refractive index detector. THF was used as eluent and the system was calibrated with polystyrene standards. Thermogravimetric analysis (TGA) was carried out under N_2 atmosphere with a heating rate of 10 °C/min up to 800 °C by using a NetzschTG 209 F1 analyzer. X-ray powder diffraction (XRD) patterns of the polymers were recorded using an X-ray diffractometer (PW 1830, Philips, Netherlands) with Cu/Kα Ni-filtered radiation at 2θ ranging from 5° to 60° in steps of 0.02°. Photoisomerization of the monomer (5.0×10^{-5} mol/L in THF) and polymers (3.8×10^{-2} g/L in THF) were measured on a Lambda 35 UV–Vis spectrophotometer (PerkinElmer, USA) against a background of THF in a quartz cuvette. The measurement was conducted at certain time intervals under irradiation with an ultraviolet lamp (15 W) at room temperature. The structural and surface morphology of the polymers on cotton fabrics were characterized by field emission scanning electron microscopy (FE-SEM) (S-4800 FE-SEM, Hitachi, Japan). The sessile drop method was used for static water contact angle measurements at ambient temperature with an automatic video contact-angle testing apparatus (Data-Physics OCA 40, DataPhysics Instruments GmbH; Germany). The average water contact angle value was determined by measuring three to five different positions of the same sample with 5 μL deionized water each time.

RESULTS AND DISCUSSION

Synthesis and Characterization of Monomer and Polymers

The fluorinated azobenzene-containing monomer (**FAzoMA**) was synthesized according to esterification reaction and diazo coupling reaction as shown in Scheme 1. The structures of the intermediate products and **FAzoMA** were characterized by ^{1}H NMR spectroscopy (as shown in Figure 1). For **FAzoMA**, the aromatic proton signals appear between 7.3 and 8.3 ppm. The signal at 6.42, 5.83 ppm and 4.70, 2.61 ∼ 2.73 ppm are due to CH_2 = C and CH_2CH_2 proton respectively. The CH_3 proton signal appears at 2.11 ppm as a strong single peak.

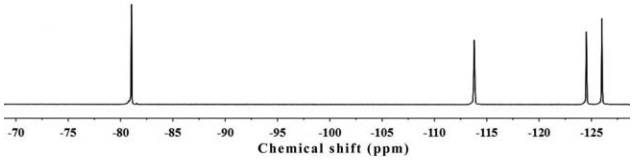

Figure 2. ^{19}F NMR spectrum of **FAzoMA**.

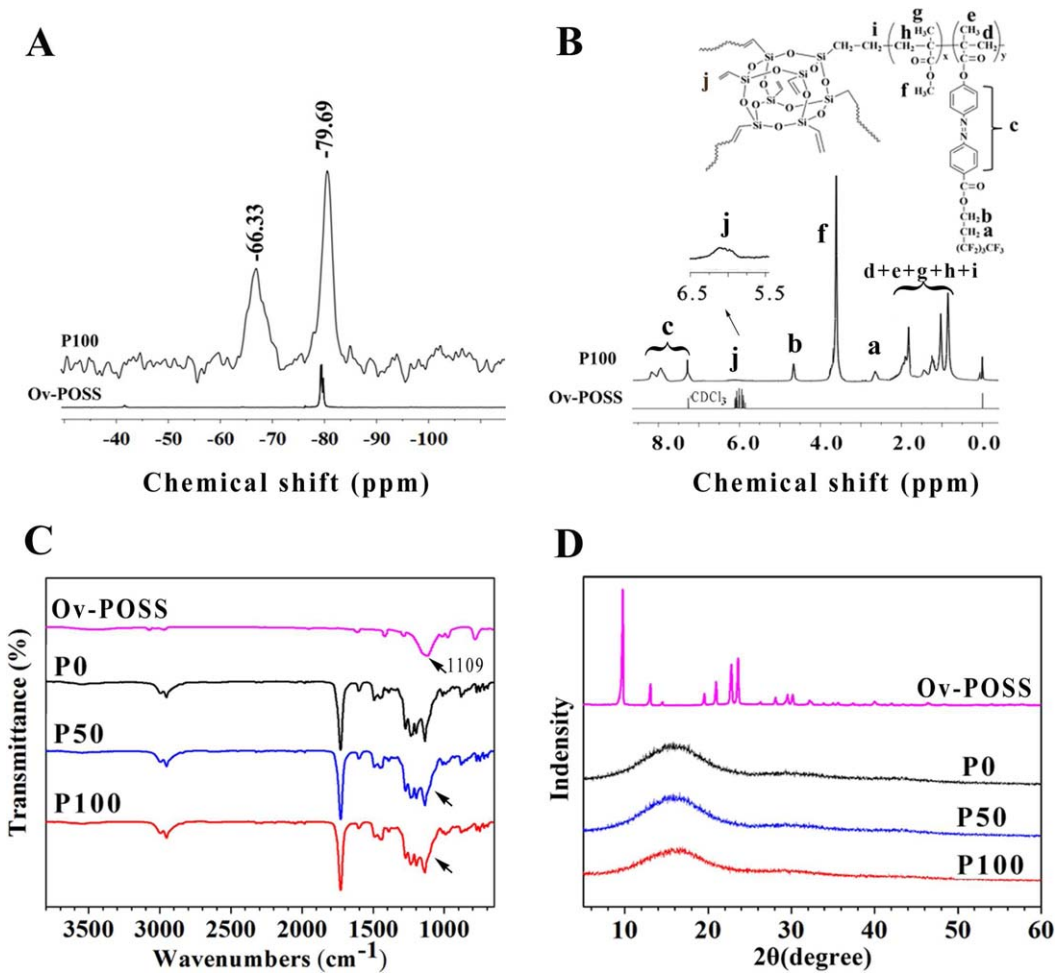

Figure 3. ^{29}Si NMR (A), ^{1}H NMR (B), FT-IR (C), and XRD (D) spectra of Ov-POSS and polymers. [Color figure can be viewed in the online issue, which is available at wileyonlinelibrary.com.]

In the ^{19}F NMR spectrum of **FAzoMA** (Figure 2), the peaks appears at about −81.0 ppm, −113.7 ppm, −124.5 ppm and −125.9 ppm are attributed to F in CF_3, CF_2 connected to CF_3 and CF_2CF_2 connected CH_2, respectively.

The POSS-based fluorinated azobenzene-containing polymer was synthesized by free radical polymerization. It was found that avoiding light during polymerization was essential to get desirable yield (more than 50%). The reason why the yield was very low (less than 5%) if without any light-avoiding procedure was probably due to the steric hindrance to the polymerization resulted from photoisomerization of azobenzene groups under light irradiation. Figure 3(A) shows the solid-state ^{29}Si NMR spectra of Ov-POSS and P(POSS-MMA-FAzoMA). The pure Ov-POSS gives only one resonance peak at −79.69 ppm since essentially all silicon atoms have the same chemical environment in the POSS molecule. The terpolymer P(POSS-MMA-FAzoMA) shows two signals at −66.33 ppm and −79.69 ppm, corresponding to Si atom connected to the reacted and unreacted vinyl groups on Ov-POSS, respectively. The appearance of new peak area at −66.33 ppm demonstrated that some vinyl groups on Ov-POSS molecule participated in the copolymerization. ^{1}H NMR spectra of Ov-POSS and P(POSS-MMA-FAzoMA) are shown in Figure 3(B). For pure Ov-POSS, the multiple resonance peaks of vinyl protons are located in the region of 5.8 ∼ 6.2 ppm. For P(POSS-MMA-FAzoMA), the weak peak at the same region indicates the existence of unreacted vinyl group in Ov-POSS segment, which is consistent with the result from ^{29}Si NMR. The residue vinyl groups provide an opportunity for introducing other functional groups into the terpolymers in further applications. The signals corresponding to the aromatic protons appear in the region of 7.0 ∼ 8.2 ppm (c). Signals at 4.66 ppm (b) and 2.65 ppm (a) are assigned to the methylene protons connected to ester and perfluoroalkyl groups in **FAzoMA** unit, respectively. The signal at 3.61 ppm (f) is attributed to methyl protons connected to ester group in MMA unit. The resonance peaks in the region of 0.5 ∼ 2.5 ppm are the overlapping proton signals of methylene groups in the terpolymers backbone and the side methyl groups in MMA unit.

The structure of terpolymers was further verified by FT-IR spectra. As shown in Figure 3(C), it can be seen clearly that the characteristic bands at 1,729 cm^{-1} and 1240 cm^{-1} of C═O and C—F are presented in all polymers. The bands at about 1600 cm^{-1}, 1500 cm^{-1} indicate the existence of aromatic rings, and the bands at 3,100–2,900 cm^{-1} are assigned to the

Table I. Effects of POSS Content on Molecular Weight and Thermal Properties of POSS-Based Terpolymers

Sample	POSS content[a] (wt %)	M_w ($\times 10^4$ g/mol)	M_n ($\times 10^4$ g/mol)	PDI	T_5[b] (°C)	T_{max} (°C)	Residue Weight[c] (%)
P0	0	2.4	1.7	1.5	210	326	6.4
P50	3.0	3.3	2.0	1.7	236	342	7.4
P100	4.7	4.3	2.5	1.7	283	340	8.9

[a] Obtained from element analysis of Si.
[b] Temperature at weight loss of 5%.
[c] Obtained from TGA.

characteristic absorbance of CH_2, CH_3 groups in the polymers. The bands at 1,100–1,276 cm^{-1} are attributed to the overlap of the characteristic Si—O—Si stretching band in POSS cage and the C—O—C stretching band in P(POSS—MMA—FAzoMA). Meanwhile, compared with **P0**, the spectra of **P50** and **P100** show the relative broadening at ~1109 cm^{-1} due to POSS incorporation into the polymers.

The microstructure of the polymers characterized by using XRD is shown in Figure 3(D). It's well known that the Ov-POSS is a highly crystalline material and has a characteristic dominant diffraction peak at $2\theta = 9.7°$.[29] It is noted that the XRD patterns of **P0**, **P50**, and **P100** exhibit amorphous structure without any peaks corresponding to Ov-POSS crystalline, indicating POSS exist in the terpolymers as polymer segments without crystalline aggregates.

The POSS-based terpolymers show good solubility in most common organic solvents as the POSS content is less than 4.7 wt %. The molecular weights (M_w and M_n) of the polymers were measured by GPC and summarized in Table I. The M_w and PDI of the polymer without POSS (**P0**) are 2.4 × 10^4 g/mol and 1.5, respectively. The molecular weights of **P50** and **P100** increase to 3.3 × 10^4 g/mol and 4.3 ×10^4 g/mol and PDI increase to 1.7 with the increase of POSS content. The opposite influences of POSS content on the molecular weights in comparison with our previous work[30] are attributed to the different POSS content range. In this study, the POSS content is less than 4.7 wt %, much lower than that of the polymers prepared in our previous work, so that small amount of POSS with eight vinyl groups here plays the role of connecting the molecule segments, which resulted in the molecule weights of the polymers increase slightly with the POSS content increase.

Thermal Properties of the Polymers

TGA was carried out to investigate the thermal behaviors of the POSS-based terpolymers. Figure 4(A) shows the weight loss of polymers when heated from ambient temperature to 800 °C under a nitrogen flow. **P0** and **P50** show a three-stage decomposition process, while **P100** shows a two-stage decomposition process. The initial decomposition of the polymers could be due to the decomposition of PMMA at the head-to-head linkages (the least stable linkages).[31] The second stage of decomposition of the polymers was due to the unsaturated chain ends and the cleavage of N=N bonds in azobenzene side chains,[31,32] and the third stage was due to the random scissions along the polymer backbone (the most stable linkages).[31] The residue char weight increased from 6.4 to 8.9 wt % when POSS content increase from 0 to 4.7 wt %. Moreover, the decomposition temperatures for 5% weight loss (T_5) of the polymers were found to be 210 °C for **P0**, 236 °C for **P50**, and 283 °C for **P100** (summarized in Table I), which shows that T_5 rises with the increase of POSS content. As seen in Figure 4(B) and Table I, the peak temperatures at which velocity of weight loss reaches maximum (T_{max}) rise from 326 °C to 340 °C when POSS content increase from 0 to 4.7 wt %. This indicates clearly that incorporation of POSS is beneficial for improving the thermal stability of the polymer.

Photo-Responsive Behavior of Monomer and Polymers

The changes in absorption of monomer and polymers in THF upon successive illumination with UV light centered on 365 nm

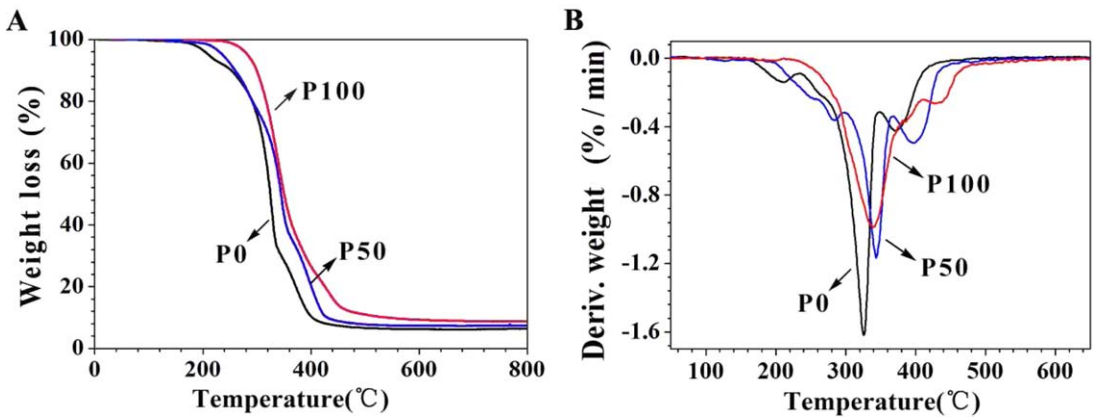

Figure 4. TGA (A) and DTG (B) curves of polymers under nitrogen. [Color figure can be viewed in the online issue, which is available at wileyonlinelibrary.com.]

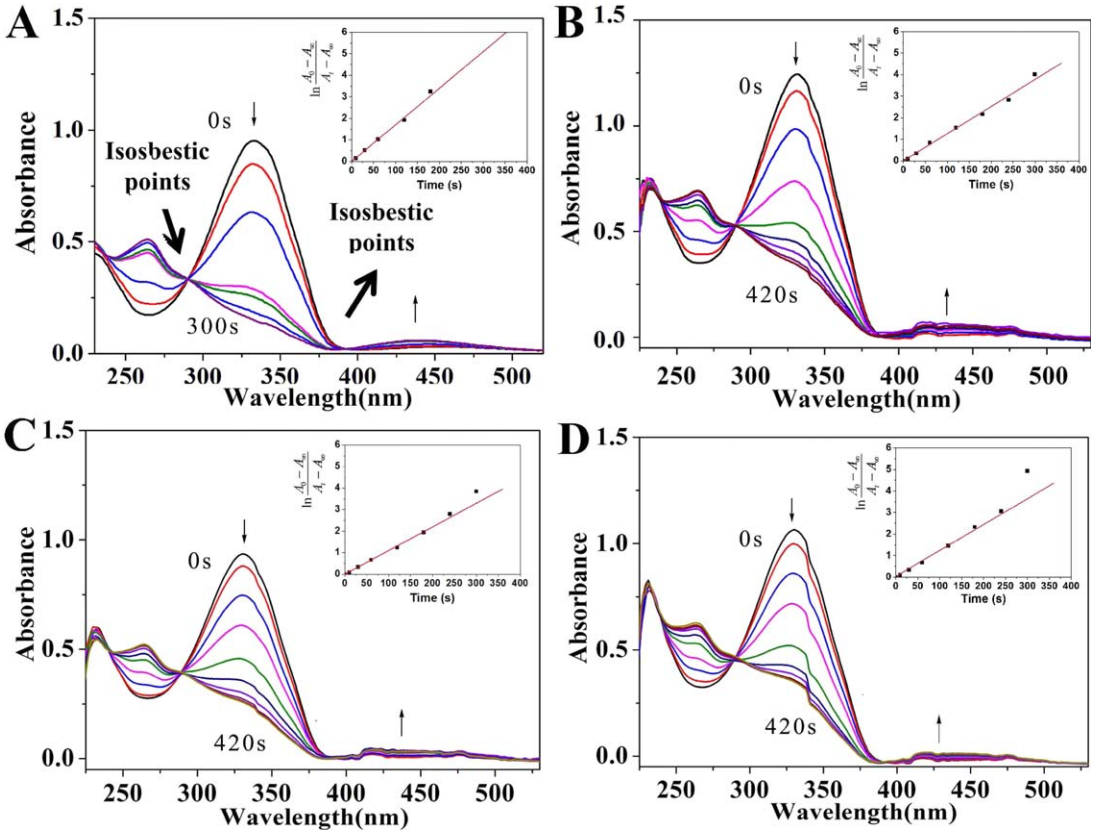

Figure 5. UV–Vis spectra of **FAzoMA** (A), **P0** (B), **P50** (C) and **P100** (D) at certain time intervals (0 s, 10 s, 30 s, 60 s, 120 s, 180 s, 300 s for **FAzoMA**; 0 s, 10 s, 30 s, 60 s, 120 s, 180 s, 240 s, 300 s, 360 s, 420 s for polymers) under UV light irradiation. Insets: the kinetics of the photoisomerization of the corresponding samples. [Color figure can be viewed in the online issue, which is available at wileyonlinelibrary.com.]

are shown in Figure 5. It's easily observed that the UV light induces the progressive decrease of absorbance band around 330 nm accompanied with the slight increase of the absorbance band around 450 nm, which is respectively attributed to the π–π^* electronic transition of *trans* configuration and the n–π^* ransition of the *cis* configuration, indicating the *trans–cis* isomerization of azo chromophores. For **FAzoMA**, as seen in Figure 5(A), photostationary state reached after UV irradiation for about 300 s. The existence of isosbestic points at about 290 and 393 nm is characteristic of the existence of two distinct absorbing species in equilibrium with each other, confirming the *trans-cis* isomerization.[16] The appearance of isosbestic points indicates that this monomolecular transformation is characterized by the presence of two spectrophotometrically distinguishable species.[33] In other words, it can be concluded that the as-synthesized azobenzene monomer is stable and neither undergoes the photo cross-linking or decomposition reaction during the high energy irradiation of UV light. The UV–Vis spectra of polymers (**P0**, **P50**, **P100**) are presented in Figure 5(B–D). Distinctly, the polymers show the similar isomerization process under the irradiation of UV light, no matter whether the POSS was incorporated or not. For the polymers, photostationary states reached after UV irradiating for about 420 s. It were reported previously that other polymers containing azobenzene groups in solution finished *trans* to *cis* isomerization under UV irradiation for about 30 minutes.[15,16] In this study, the synthesized polymers in THF solution finished *trans* to *cis* photoisomerization within only several minutes. At present, there are three isomerization mechanisms on the *trans-cis* photoisomerization of azobenzene: rotation, inversion and concerted-inversion mechanisms.[34] For the substituted azobenzene, the non-nitro-substituted species are more likely to follow an inversion mechanism.[35] The previous work reported that the electron-withdrawing groups favor the inversion pathway[36] due to the strong electron-withdrawing substituent decreasing the barrier to isomerization by reducing the double-bond character of the azo group.[34] In our study, the carbonyl group connected to azobenzene as an electro-withdrawing substituent might play the role of lowering energy barrier, resulting in the relatively fast isomerization.

Kinetics of the photoisomerization processes were analyzed by the first-order kinetics expression in eq. (1).[37,38]

$$\ln \frac{c_0 - c_\infty}{c_t - c_\infty} = k_c t \quad (1)$$

As A $\propto$ c

So,

$$\ln \frac{A_0 - A_\infty}{A_t - A_\infty} = kt \quad (2)$$

Where A_t, A_0, and A_∞ are the absorbance at λ_{max} at time t, time zero, and infinite time, respectively. Based on the

Table II. Kinetics Constants of **FAzoMA** and Polymers

Sample	**FAzoMA**	P0	P50	P100
kinetics constant (s^{-1})	1.70×10^{-2}	1.26×10^{-2}	1.10×10^{-2}	1.20×10^{-2}

first-order kinetic plots according to eq. (2) for **FAzoMA**, **P0**, **P50** and **P100**, it was found that the reactions proceed in the first order kinetics in THF solution within 250 seconds and then deviated from the first-order kinetics to some extent (seen in Figure 5 insets).

The kinetics constants of **FAzoMA** and polymers are listed in Table II. As expected, the photoisomerization rates of the polymers are lower than that of **FAzoMA** because the movements of azobenzene groups are affected by the polymer structure. Comparing **P0**, **P50** and **P100**, the photoisomerization rates of them seem to be in the same range ($1.2 \pm 0.1 \times 10^{-2}$ s^{-1}). It indicated that the photoisomerization of the polymers almost were not influenced by the steric hindrance of POSS when POSS content less than 4.7 wt %.

Surface Morphology and Wettability of the Coated Fabrics

The surfaces morphology of the cotton fabric untreated and treated with **P0**, **P50**, or **P100** were observed by FE-SEM and shown in Figure 6. The FE-SEM image of the pristine cotton fabric shows the relative plain surface except some natural texture [Figure 6(A)]. On the surface of cotton fabric coated with **P0**, polymer layer appears [noted by arrow on Figure 6(B)]. As shown on the surface of **P50** coated fabric [Figure 6(C)], some white dots caused by POSS agglomeration are observed. The surface of **P100** coated fabric shows more white dots or big convexes [Figure 6(D)], which means more POSS polymerized in the polymer.

The hydrophobicity of the coated cotton fabric surfaces were assessed with water contact angle (CA) measurements. The data summarized in Table III show that water CA increases with the increasing of POSS content. The water CAs of the fabrics coated with **P0** (~ 142 °), **P50** (~ 146 °), and **P100** (~152 °) indicate that hydrophobicity of the coated cotton fabrics are improved by the addition of POSS. The surface of the cotton fabrics coated with **P100** exhibits the roughest morphology [seen in Figure 6(D)] and from which superhydrophobicity achieves (water CA higher than 150 °).[39] After being adequately exposed to UV light for about 15 minutes, the water CAs of the fabrics coated with **P0**, **P50** and **P100** decreased to 135 ° ~ 137 ° (as seen in Table III and Figure 7). The water CA of **P100** coated fabric changed 15 °, and that of **P0**, **P50** treated fabrics changed 7 ° and 10 ° respectively. The changes of water CA resulted from the photoisomerization of the azobenzene groups, which was basically in accordance with our anticipation.

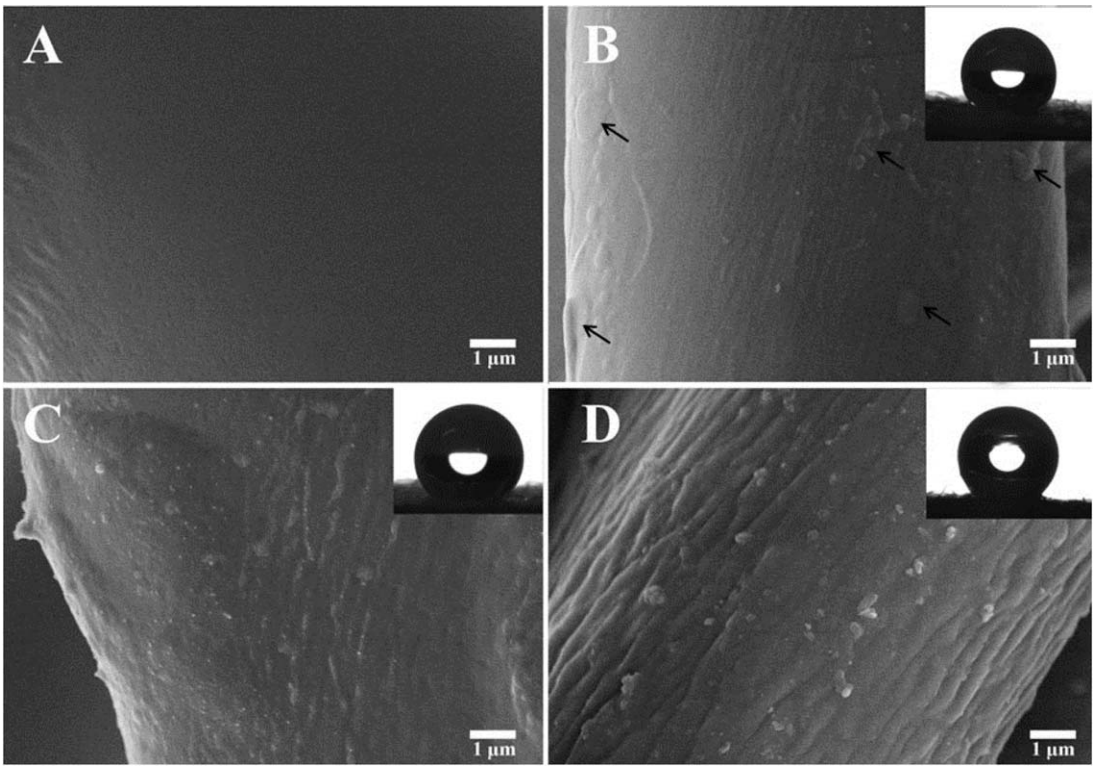

Figure 6. FE-SEM images of the surfaces of uncoated fabric (A) and fabrics coated with **P0** (B), **P50** (C) and **P100** (D). Insets: photos of water droplets on the corresponding samples.

Table III. Effects of POSS Content and UV Light Irradiation on the Water CAs of the Coated Fabrics

Coated polymer	POSS content (wt %)	Water CA (before irradiation) (°)	Water CA (after irradiation) (°)	Water CA change (°)
P0	0	142 ± 2	135 ± 1	7
P50	3.0	146 ± 3	136 ± 2	10
P100	4.7	152 ± 1	137 ± 1	15

We have to point out that without any extra surface fabrication, the changes of water CAs from the POSS-based polymers coated cotton fabrics are relatively small compared to the results from the surfaces modified by anisotropic etching[40] or nanotechnology.[41] In this study we focus on the preparation, characterization and photoisomerization behavior of **FAzoMA** and its POSS-based polymer. The influences of surface structure on the POSS-based polymer wettability will be undertaken in the next study.

CONCLUSIONS

A polymerizable fluorinated azobenzene-containing monomer and its POSS-based polymer were successfully prepared and well characterized. The thermal stability of the polymers was improved by polymerization of POSS, while the photoisomerization of the polymers almost were not influenced by the steric hindrance of POSS in our study range. The UV–Vis absorption spectra demonstrated that the monomer and the polymers possessed similar photoisomerization behavior and the same order of magnitude of the first-order kinetics constant (10^{-2} s). Furthermore, the terpolymer-coated cotton fabrics achieved superhydrophobicity when POSS content at about 4.7 wt %, and the water wettability changed with irradiation of UV light. The POSS-based photoresponsive polymer is potential to be developed for a wide range of fields requiring external stimuli-responsive surface.

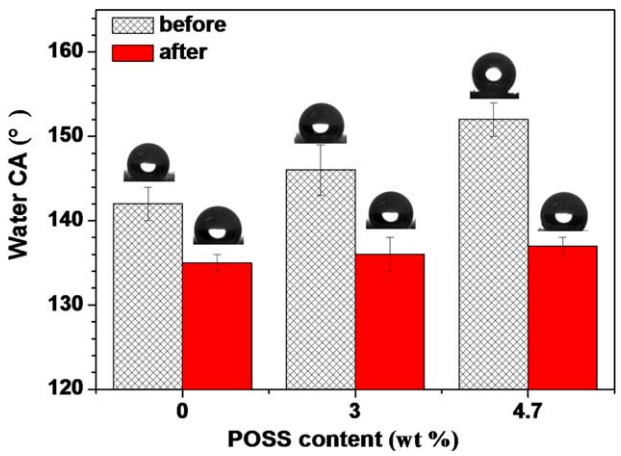

Figure 7. Effects of POSS content on the wettability of the coated fabrics before and after UV irradiation. [Color figure can be viewed in the online issue, which is available at wileyonlinelibrary.com.]

ACKNOWLEDGMENTS

The authors are grateful for the financial supports from the National Natural Science Foundation of China (51203021, 31271028), Innovation Program of Shanghai Municipal Education Commission (13ZZ051) and Chinese Universities Scientific Fund (CUSF-DH-D-2015043).

REFERENCES

1. Yu, X.; Wang, Z.; Jiang, Y.; Shi, F.; Zhang, X. *Adv. Mater.* **2005**, *17*, 1289.
2. Minko, S.; Muller, M.; Motornov, M.; Nitschke, M.; Grundke, K.; Stamm, M. *J. Am. Chem. Soc.* **2003**, *125*, 3896.
3. Xu, L.; Chen, W.; Mulchandani, A.; Yan, Y. *Angew. Chem. Int. Ed.* **2005**, *44*, 6009.
4. Krupenkin, T.; Taylor, J.; Wang, E.; Kolodner, P.; Hodes, M.; Salamon, T. *Langmuir* **2007**, *23*, 9128.
5. Ichimura, K.; Oh, S.; Nakagawa, M. *Science* **2000**, *288*, 1624.
6. Caputo, G.; Cortese, B.; Nobile, C.; Salerno, M.; Cingolani, R.; Gigli, G.; Cozzoli, P.; Athanassiou, A. *Adv. Funct. Mater.* **2009**, *19*, 1149.
7. Kamegawa, T.; Shimizu, Y.; Yamashita, H. *Adv. Mater.* **2012**, *24*, 3697.
8. Feng, X.; Feng, L.; Jin, M.; Zhai, J.; Jiang, L.; Zhu, D. *J. Am. Chem. Soc.* **2004**, *126*, 62.
9. Xin, B.; Hao, J. *Chem. Soc. Rev.* **2010**, *39*, 769.
10. Browne, W.; Feringa, B. *Annu. Rev. Phys. Chem.* **2009**, *60*, 407.
11. Klajn, R. *Pure Appl. Chem.* **2010**, *82*, 2247.
12. Nachtigall, O.; Kordel, C.; Urner, L.; Haag, R. *Angew. Chem. Int. Ed.* **2014**, *53*, 9669.
13. Abrakhi, S.; Peralta, S.; Fichet, O.; Teyssie, D.; Cantin, S. *Langmuir* **2013**, *29*, 9499.
14. Feng, C.; Zhang, Y.; Jin, J.; Song, Y.; Xie, L.; Qu, G.; Jiang, L.; Zhu, D. *Langmuir* **2001**, *17*, 4593.
15. Tang, Q.; Meng, X.; Jiang, H.; Zhou, T.; Gong, C.; Fu, X.; Shi, S. *J. Mater. Chem.* **2010**, *20*, 9133.
16. Pei, X.; Fernandes, A.; Mathy, B.; Laloyaux, X.; Nysten, B.; Riant, O.; Jonas, A. *Langmuir* **2011**, *27*, 9403.
17. Xue, Y.; Wang, H.; Yu, D.; Feng, L.; Dai, L.; Wang, X.; Lin, T. *Chem. Commun.* **2009**, 6418.
18. Li, G.; Wang, L.; Ni, H.; Pittman, C. *J. Inorg. Organomet. Polym.* **2001**, *11*, 123.

19. Phillips, S.; Haddad, T.; Tomczak, S. *Curr. Opin. Solid State Mater. Sci.* **2004**, *8*, 21.
20. Pielichowski, K.; Njuguna, J.; Janowski, B.; Pielichowski. *J. Adv. Polym. Sci.* **2006**, *201*, 225.
21. Tuteja, A.; Choi, W.; Ma, M.; Mabry, J.; Mazzella, S.; Rutledge, G.; McKinley, G.; Cohen, R. *Science* **2007**, *318*, 1618.
22. Xu, J.; Li, X.; Cho, C.; Toh, C.; Shen, L.; Mya, K.; Lu, X.; He, C. *J. Mater. Chem.* **2009**, *19*, 4740.
23. Ellis, D.; Mabury, S.; Martin, J.; Muir, D. *Nature* **2001**, *412*, 321.
24. Keil, D.; Mehlmann, T.; Butterworth, L.; Peden-Adams, M. *Toxicol. Sci.* **2008**, *103*, 77.
25. Mulkiewicz, E.; Jastorff, B.; Skladanowski, A. C.; Kleszczynski, K.; Stepnowski, P. *Environ. Toxicol. Pharm.* **2007**, *23*, 279.
26. Barmentlo, S. H.; Stel, J. M.; van Doom, M.; Eschauzier, C.; de Voogt, P.; Kraak, M. H. S. *Environ. Pollut.* **2015**, *198*, 47.
27. Hosangadi, B.; Dave, R. *Tetrahedron Lett.* **1996**, *37*, 6375.
28. Yoshino, N.; Kitamura, M.; Seto, T.; Shibata, Y.; Abe, M.; Ogino, K. B. *Chem. Soc. Jpn.* **1992**, *65*, 2141.
29. Wang, R.; Wang, S.; Zhang, Y. *J. Appl. Polym. Sci.* **2009**, *113*, 3095.
30. Gao, Y.; He, C. L.; Huang, Y. G.; Qing, F. L. *Polymer* **2010**, *51*, 5997.
31. Hussain, H.; Mya, K.; Xiao, Y.; He, C. *J. Polym. Sci. Part A: Polym. Chem.* **2008**, *46*, 766.
32. Rameshbabu, K.; Kannan, P. *Polym. Int.* **2006**, *55*, 151.
33. Frenz, C.; Fuchs, A.; Schmidt, H.; Theissen, U.; Haarer, D. *Macromol. Chem. Physic* **2004**, *205*, 1246.
34. Crecca, C. R.; Roitberg, A. E. *J. Phys. Chem. A* **2006**, *110*, 8188.
35. Ho, C. H.; Yang, K. N.; Lee, S. N. *J. Polym. Sci. Part A: Polym. Chem.* **2001**, *39*, 2296.
36. Angelini, G.; Canilho, N.; Emo, M.; Kingsley, M.; Gasbarri, C. *J. Org. Chem.* **2015**, *80*, 7430.
37. Mita, I.; Horie, K.; Hirao, K. *Macromolecules* **1989**, *22*, 558.
38. Naito, T.; Horie, K.; Mita, I. *Polymer* **1993**, *34*, 4140.
39. Wang, S.; Jiang, L. *Adv. Mater.* **2007**, *19*, 3423.
40. Groten, J.; Bunte, C.; Ruhe, J. *Langmuir* **2012**, *28*, 15038.
41. Lim, H.; Lee, W.; Lee, S.; Lee, D.; Jeon, S.; Cho, K. *Chem. Commun.* **2010**, *46*, 4336.